Numerical, Laboratory And Field Studies of Gas Production From Natural Hydrate Accumulations in Geologic Media

George J. Moridis, Timothy Kneafsey, Michael Kowalsky and Matthew Reagan

Lawrence Berkeley National Laboratory, Berkeley, USA

ABSTRACT: We discuss the range of activities at Lawrence Berkeley National Laboratory in support of gas production from natural hydrates. Investigations of production from the various classes of hydrate deposits by numerical simulation indicate their significant promise as potential energy sources. Laboratory studies are coordinated with the numerical studies and are designed to address knowledge gaps that are important to the prediction of gas production. Our involvement in field tests is also briefly discussed.

Key words: hydrates, gas production, simulation, laboratory studies, field studies

1. INTRODUCTION

1.1. Background

Gas hydrates are solid crystalline compounds in which gas molecules are lodged within the lattices of ice crystals. Natural gas hydrate deposits involve mainly CH_4, and occur in two distinctly different geologic settings: in the permafrost and in deep ocean sediments. Current estimates of CH_4 in hydrates vary widely, ranging between 10^{15} to 10^{18} m^3 (Sloan, 1998). The most conservative estimate surpasses by a factor of two the energy content of all conventional fossil fuel reserves. Thus, hydrates are attracting attention as a potential energy resource. Gas from hydrates can be produced by inducing dissociation by any combination of the following three main methods: (1) depressurization, (2) thermal stimulation, and (3) the use of hydration inhibitors (e.g., salts and alcohols).

1.2. Classification of Hydrate Deposits

Natural hydrate accumulations are divided into four classes (Moridis and Collett, 2003; Moridis and Sloan, 2006). Class 1 accumulations are composed of two layers: an underlying two-phase fluid zone with free (mobile) gas, and an overlying hydrate-bearing layer (HBL) involving water and hydrate (Class 1W) or gas and hydrate (Class 1G). In Class 1 deposits, the bottom of the hydrate stability zone coincides with the bottom of the hydrate interval. Class 2 deposits comprise two zones: the HBL overlying a mobile water zone. Class 3 accumulations are composed of a single zone, the HBL, and are

characterized by the absence of an underlying zone of mobile fluids. In Classes 2 and 3, the entire hydrate interval may be at or within the hydrate stability zone. Finally, Class 4 deposits involve disperse, low-saturation accumulations in marine geologic media that are not bounded by confining strata and can extend over large areas.

1.3. Purpose

The purpose of this paper is to summarize the studies conducted at the Lawrence Berkeley National Laboratory (LBNL), Berkeley, USA, in support of gas production from natural gas hydrates in geological media. These studies include numerical analyses of the gas production potential of the various classes of hydrate deposits, and laboratory investigations to determine important parameters and relationships describing the kinetic, hydraulic and thermal behavior of hydrate-bearing sediments. Finally, the LBNL studies in support of field tests of gas production from hydrates are briefly discussed.

2. NUMERICAL STUDIES

2.1. The Numerical Simulator

The numerical studies were conducted using the TOUGH-Fx/HYDRATE simulator (Moridis et al., 2005a), which can simulate the non-isothermal hydration reaction, phase behavior and flow of fluids and heat in natural CH_4-hydrate deposits. It includes both an equilibrium and a kinetic model of hydrate dissociation, and accounts for heat and up to four mass components (i.e., water, CH_4, hydrate, and water-soluble inhibitors such as salts or alcohols) which are partitioned among four possible phases: gas, aqueous, ice, and hydrate. A total of 13 states (phase combinations) can be described, involving any combination of hydrate dissociation mechanisms.

2.2. Case 1: Gas Production From Class 1W Deposits

Class 1 appears to be a promising target for gas production because the thermodynamic proximity to the hydration equilibrium requires only small changes in P and T to induce dissociation (Moridis and Collett, 2003; Moridis et al., 2005b). Additionally, the existence of a free gas zone guarantees gas production even when the hydrate contribution is small. The Class 1W deposit in Case 1 involves a 15m-thick HBL, in which the hydrate saturation $S_H = 0.7$ and the aqueous saturation $S_A = 0.3$. The HBL is underlain by a 15m-thick zone of mobile gas and water. The reservoir radius is $R_{max} = 567.5$ m and its intrinsic permeability $k = 10^{-12}$ m^2 (=1 Darcy). At the bottom of the HBL, the initial $P = 1.067 \times 10^7$ Pa and $T = 286.65$ K, and the P and T distributions in the profile follow the

hydrostatic and geothermal gradients, respectively. Gas is produced by depressurization through a heated well at the center of the reservoir at a rate of $Q = 0.82$ ST m^3/s.

To describe gas production from Class 1 hydrates, we employ the concepts of *Rate Replenishment Ratio* (RRR, defined as the fraction of the gas production rate Q_P that is replenished by CH_4 from hydrate dissociation) and *Volume Replenishment Ratio* (VRR, i.e., the fraction of the cumulative produced CH_4 volume V_P that has been replenished by CH_4 from hydrates), as proposed by Moridis et al. (2005b). The evolution of the volumetric rate of CH_4 release from the hydrate (Q_R) and of the corresponding Q_P are shown in Figure 1a. We identify four stages (Figure 1b). Stage I corresponds to dissociation from two zones: the initial horizontal hydrate interface and a cylindrical interface around the well. A second horizontal hydrate interface evolves at the top of the hydrate interval. Additionally, a *hydrate channeling* system begins to evolve. This is composed of narrow conductive channels alternating with impermeable high-S_H bands that advance into the body of the hydrate in a 'wormhole-like" manner aligned with the general direction of flow. This is a consequence of the hydrate lensing process caused by capillary pressure (Moridis et al., 2005b), and provides access to the hydrate interior.

In Stage II, dissociation is at its maximum and occurs along the two horizontal interfaces (upper and lower) and the cylindrical interface, while the hydrate channels are fully developed. The end of Stage II is marked by a precipitous drop in RRR caused by the "sealing" of the entire bottom (horizontal) boundary by an impermeable hydrate lens of a very high S_H, in which S_A and S_G fall below their irreducible levels. In Phase III, only the cylindrical and the upper horizontal interfaces are active dissociation fronts.

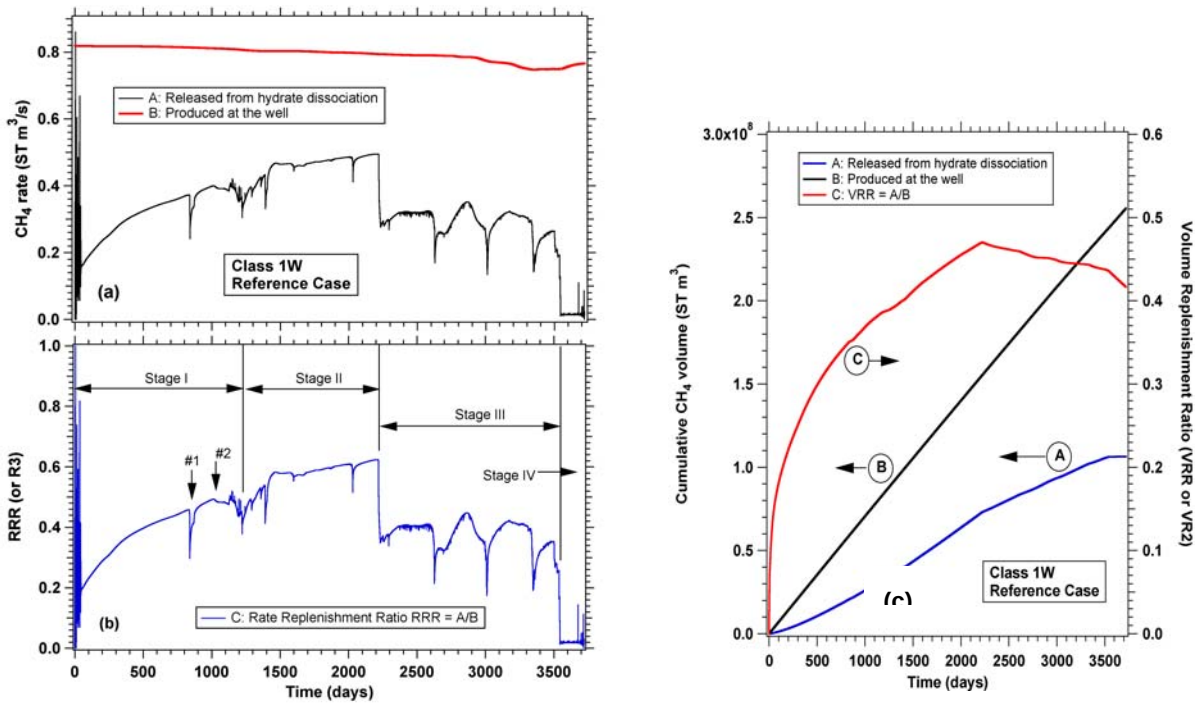

Fig. 1. (a) Evolution of Q_R (A) and Q_P (B), (b) the corresponding RRR (C) during production from the Class 1W deposit; (c) evolution of V_R (A), V_P (B) and the corresponding VRR (C) (Moridis et al., 2005b).

The dissociation zone created by the hydrate channels is also active, but *hydrate lensing* (Moridis et al., 2005b) leads to increasing S_H, thus reducing the aperture of the "wormholes". Compared to Stages I and II, RRR is lower in Stage III and has a downward trend because (a) the total area of dissociation is reduced after the occlusion of the bottom interface, (b) the remaining dissociating regions are more distant from the well, and (c) the cross-sectional area of the hydrate channels decreases. The onset of Stage IV is marked by another precipitous drop in the RRR value to levels below 0.1. This indicates a dramatic reduction in dissociation activity and is caused by occlusion of the upper interface, or through closure of the hydrate channels (Moridis et al., 2005b). In Figure 1a and 1b we observe that Q_R attains high levels early, and it increases with time in Stage I and II. At the end of Phase II (t = 6.2 years), Q_R = 0.533 ST m^3/s and replenishes about 65% of Q_P. Even with the decline in Q_R in Stage III, RRR averages about 40%. Comparison of the cumulative volume of CH_4 released from dissociation (V_R) to V_P leads to the VRR shown in Figure 1c, which confirms the hydrate potential as a promising gas source. At the end of the 10-year production period, VRR = 0.42, i.e., 42% of the total gas produced volume (1.08x10^8 ST m^3) has been replenished from dissociation. The corresponding water production is limited (Moridis et al., 2005b). These results indicate the technical feasibility of depressurization to readily produce large amounts of gas at high rates using conventional technology.

Figure 2 shows the distribution of S_H over time. Figure 2b reveals the expansion of the cylindrical interface radially from the wellbore during Stage I. The upper interface becomes evident after t = 4 years, i.e., at the beginning of Stage II (Figure 2c). The emergence of the banded S_H distribution of the hydrate channels is also obvious, which becomes more pronounced with time as they advance into the hydrate body. The hydrate channels are evident at t = 4 years. These "wormhole-like" structures appear to permeate a large portion of the main hydrate body during Stage III (t = 6 years, Figure 2e) and an even larger one in Stage IV (Figure 2f, t = 10 years).

2.3. Case 2: Gas Production From Class 1G Deposits

The system configuration, geometry, and properties in this case are similar to those in the Class 1W case, from which it differs in that in the HBL, S_H = 0.7 and S_G = 0.3. The (a) volumetric rate of depressurization-induced CH_4 release from the hydrate, (b) the production rate at the well, and (c) the corresponding RRR appear in Figure 3a (Moridis et al., 2005b). This figure shows that dissociation from hydrates in Class 1G deposits is a continuous process that does not have the stages identified in Class 1W deposits (Figure 1). The hydrate contribution to production increases monotonically with time, and RRR = 0.75 at the end of the 30-year production period. Comparison of V_R and V_P leads to the VRR in Figure 2b, which rises rapidly early, increases continuously with time, and shows that 54% of the produced volume at the end of the 30-year production period has been replenished from hydrate dissociation. By that time, 4.13×10^8 ST m^3 have been released from dissociation. These results further confirm the technical feasibility of depressurization to produce large amounts of gas from hydrates at high rates using conventional technology. The attractiveness of Class 1G deposits is further enhanced by low water production (Moridis et al., 2005b).

2.4. Case 3: Gas Production From a Class 2 Deposit

The geometry of the Class 2 deposit discussed here is as in Case 1, from which it differs in that the zone underneath the HBL is water-saturated. Fluids are produced through a single well at the center of the reservoir at a constant rate of Q = 9.48 kg/s (5000 BPD). The producing interval extends from the top of the HBL to 7 m below its base.

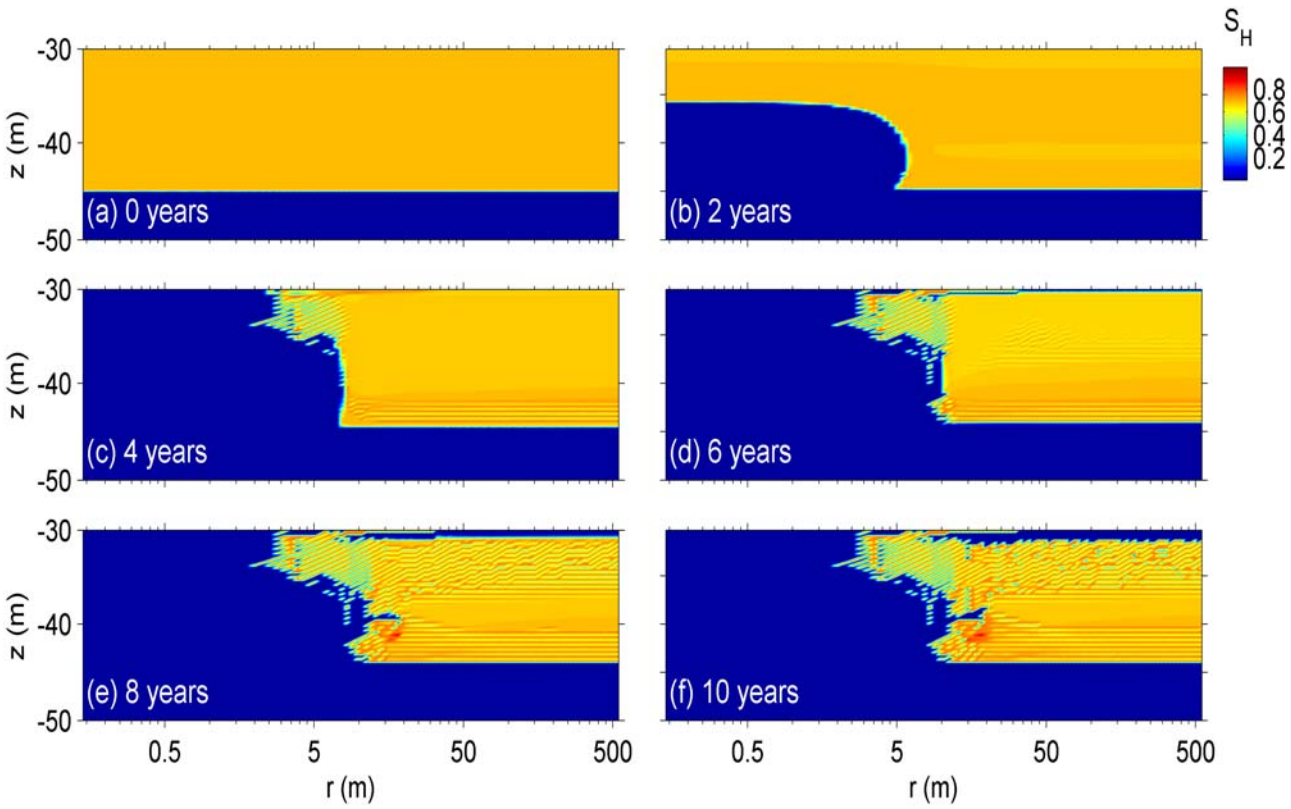

Fig. 2. Evolution of the hydrate saturation distribution during depressurization-induced gas production from a Class 1W hydrate deposit (Moridis et al., 2005b).

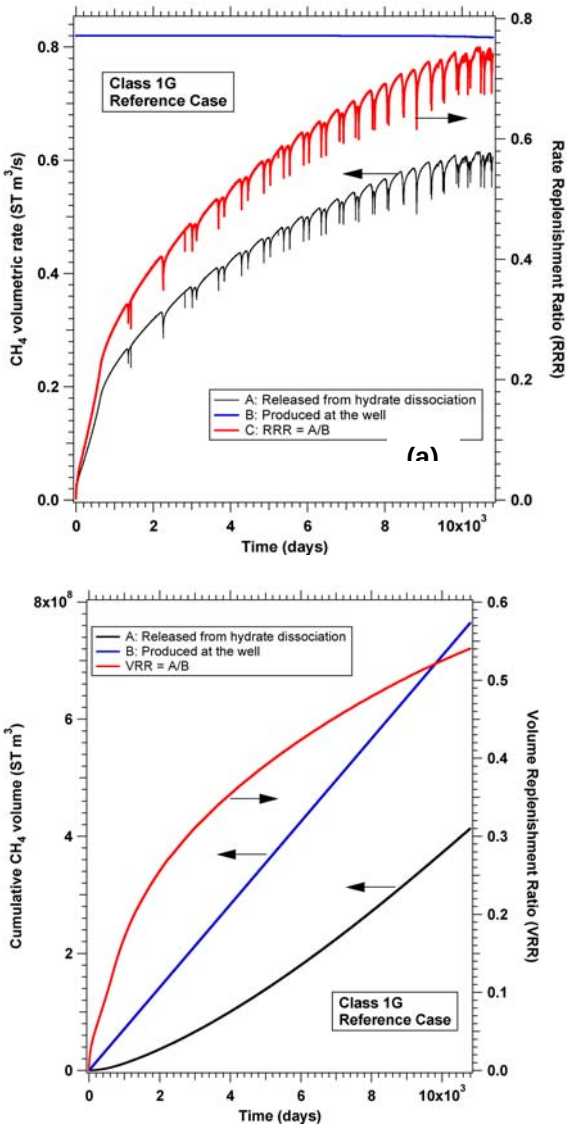

Fig. 3. (a) Evolution of Q_R (A), Q_P (B), and the corresponding RRR (C) from a Class 1G hydrate deposit; (b) evolution of V_R (A), V_P (B) and the corresponding VRR (C).

Figure 4a shows the evolution of (a) the rate Q_R of CH_4 release from hydrate dissociation into the reservoir, and (b) the rate Q_P of CH_4 production at the well. In Class 2 hydrate deposits, $Q_R > Q_P$ because of the need for gas to accumulate until S_G exceeds the irreducible S_{irG} before flowing to the well. Because of the very low compressibility of water, the depressurization effect is immediate, and leads to the release of large volumes of CH_4. Figure 4a shows two stages, separated by a 30-day period of warm water injection to eliminate the secondary hydrate that forms near the wellbore. Gas production is zero and gas release from the hydrate is minimal during this period, which is followed by a decrease in the well Q upon the resumption of production (to avoid cavitation). Q_R increases monotonically during each of the two stages. Although it takes some time before a substantial CH_4 production is observed at the well, Q_P continues to increase and

to converge toward Q_R during the study period. At t = 5 years, Q_P reaches the very attractive level of 4.4 ST m^3/s (i.e., about 4.4x10^6 ST ft^3/day), at which time V_P = 1.3x10^8 ST m^3 (4.62x10^9 ST ft^3, Figure 4b). This very large volume of produced gas indicates the attractiveness of Class 2 deposits as potential energy sources.

The S_G distribution at t = 5 years in Figures 5a shows the presence of two sizeable gas banks above and below the hydrate body. The corresponding S_H distribution in Figure 5b shows the formation of secondary hydrate near the wellbore. The two free gas zones (Figure 5a) extend along the entire reservoir radius, and are typical of hydrate deposit dissociation. Figures 5a and 5b show that gas from the two zones moves downward under the protruding secondary hydrate structure to reach the well and allow production.

2.5. Effect of Boundaries on Production From a Class 2 Deposit

The effect of boundaries on gas production from Class 2 deposits can be significant. Moridis and Kowalsky (2006) showed that the presence of a permeable overburden and a deep water zone can reduce gas production from Class 2 hydrate deposits to very low levels that are orders of magnitude lower than those indicated in Figure 4 and are further encumbered by large water production. This disappointing performance is caused by the reduced effectiveness of depressurization in the presence of permeable boundaries and deep-water zones, and indicates that simple depressurization is not a promising production method from this kind of Class 2 deposits. The same authors also determined that

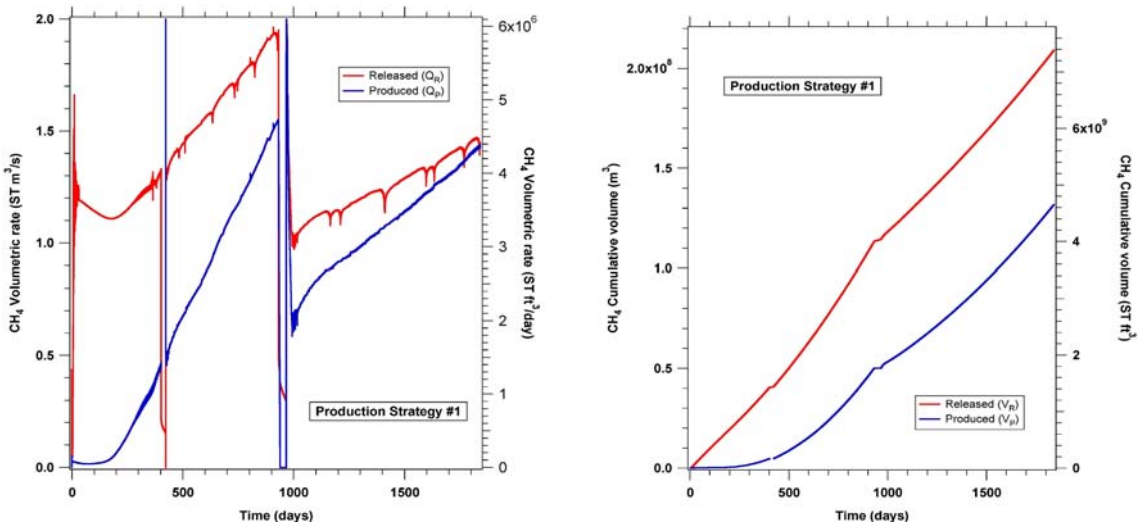

Fig. 4. (a) Evolution of Q_R and Q_P, and (b) V_R and V_P during production from a Class 2 hydrate deposit.

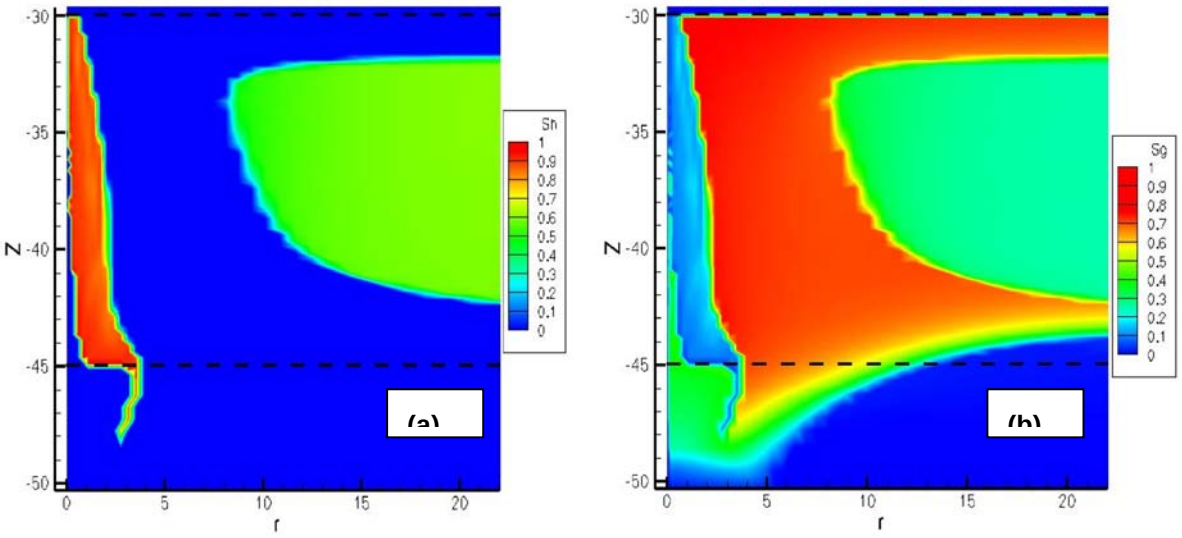

Fig. 5. Distributions of (a) S_H and (b) S_G near the wellbore during production from a Class 2 hydrate deposit.

five-spot production methods involving hot water injection do not seem to lead to substantial gas production, a situation they attributed to the adverse effect of water injection on the magnitude of depressurization (induced by the production wells).

2.6. Case 5: Gas Production From a Class 3 Deposit

Case 5 involves a 25 m-thick hydrate deposit of $k = 3\text{x}10^{-13}$ m^2 that is bounded by an impermeable shale overburden and overburden. Two production methods are explored. The first is based on thermal stimulation, and is appropriate when S_H is too high (> 0.65) to allow sufficient flow and depressurization. The second method is based on depressurization, and is applicable to Class 3 deposits with sufficient residual permeability (typically involving S_H < 0.5). The simulation results indicate that Q_P from thermal stimulation (induced by the circulation of warm water at the well at T_w = 50 ^{o}C) is generally very low (< 50 ST m^3/day, see Figure 6a), and orders of magnitude below the level of commercial viability. Despite a lower S_H, Q_P from the depressurization of Class 3 deposits (induced by a well Q = 15 kg/s) is much higher than that for thermal stimulation ($6\text{x}10^3$ to $1.6\text{x}10^4$ ST m^3/day, see Figure 6b), but remains significantly below generally accepted standards of commercially viability.

2.7. Gas Production From a Class 4 Deposit

Moridis and Sloan (2006) investigated the subject of gas production from Class 4 hydrate deposits, involving disperse, low-S_H accumulations in oceanic sediments. Despite covering the spectrum of expected variations in system properties, initial conditions, and operational parameters, their results indicated very low gas production volumes that are further encumbered with large water production. Moridis and Sloan (2006) were unable to identify conditions leading to economically viable gas production, and reached the conclusion that Class 4 deposits are not promising targets for gas production.

3. LABORATORY STUDIES

The numerical studies discussed in Section 2 indicated the importance of several properties and processes that play important roles in our understanding and the accuracy of predicting of gas production from natural hydrate deposits. The processes in question are heat and mass transfer, and the properties of interest include the following: kinetic parameters of hydrate dissociation, composite thermal conductivity, composite specific heat, relative permeability k_r, and capillary pressure P_c of hydrate-bearing media. Information on these subjects is scant. The laboratory studies at LBNL are designed to address these knowledge gaps, and are closely coordinated with the numerical studies.

An important feature of the LBNL laboratory studies is the extensive use of x-ray computed tomography (CT) scanning, in addition to the conventional monitoring of P, T, and gas rates, volumes and composition. The need for CT scanning stems from the significant heterogeneity (spatial and temporal) of the hydrate distribution in the porous media during dissociation. Visualization prevents the misinterpretation of localized phenomena as a volume-averaged process. The complexity of the coupled processes

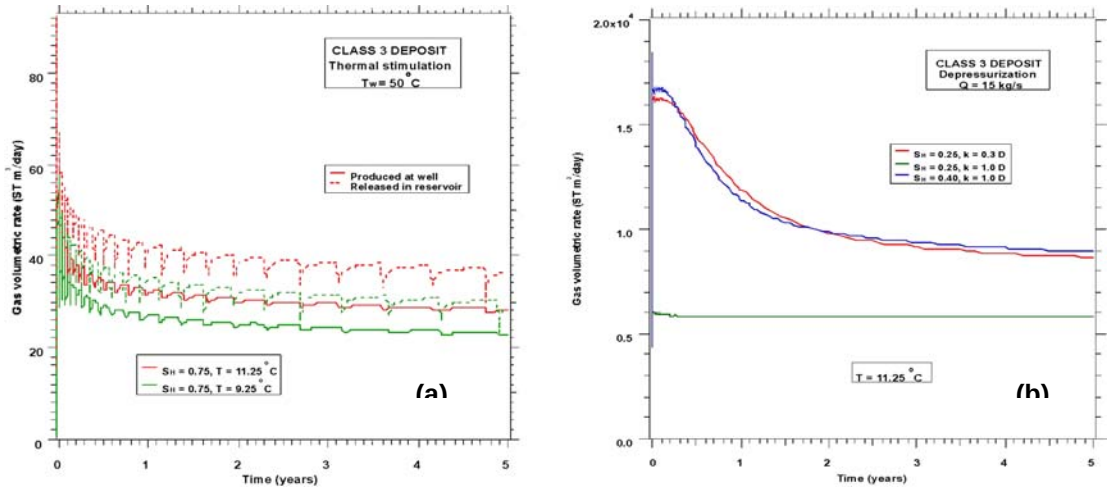

Fig. 6. Evolution of Q_R and Q_P during gas production from Class 3 hydrate deposits: (a) thermal stimulation, and (b) depressurization.

involved in hydrate dissociation (thermal, thermodynamic, and hydraulic) precludes the use of simple measurements as the means to determine the parameters and relationships of interest, and instead necessitates the use of inverse modeling (history matching).

Figure 7 shows some of the equipment involved in the process of determining the kinetic parameters of hydrate dissociation and the thermal properties of hydrate bearing sediments (i.e., composite thermal conductivity and specific heat), including the pressure vessel, *P* and *T* monitoring equipment, and the x-ray CT scanner (Kneafsey et al., 2005; Gupta et al., 2006). The attached curves show the agreement between measurements and predictions based on the optimized parameters obtained from inverse modeling (Moridis et al., 2005c). Figure 8 shows the longitudinal x-ray scan of the high-*P* vessel used for k_r studies (currently in progress), a cross-sectional scan of a waterflooding experiment, in addition to the corresponding attenuation curves that are used for the extraction of the k_r parameters. Finally, Figure 9 shows the Advanced Light Source facility at LBNL, in which the availability of the most powerful x-rays in the world makes possible the use of synchrotron-based CT microtomography to investigate fundamental processes of the hydration reaction in porous media (e.g., the site of hydrate formation in the pores and the derivation of k_r and P_c relationships from pore-level structural data).

4. ANALYSES IN SUPPORT OF FIELD STUDIES

LBNL staff were involved in the design of the first field test of gas production from hydrates, conducted at the Mallik site, Mackenzie Delta, Northwest Territories, Canada, in 2002 (Moridis et al., 2004). Analysis of the field data and long-term predictions of gas production from the Mallik site can be found in Moridis et al. (2005d).

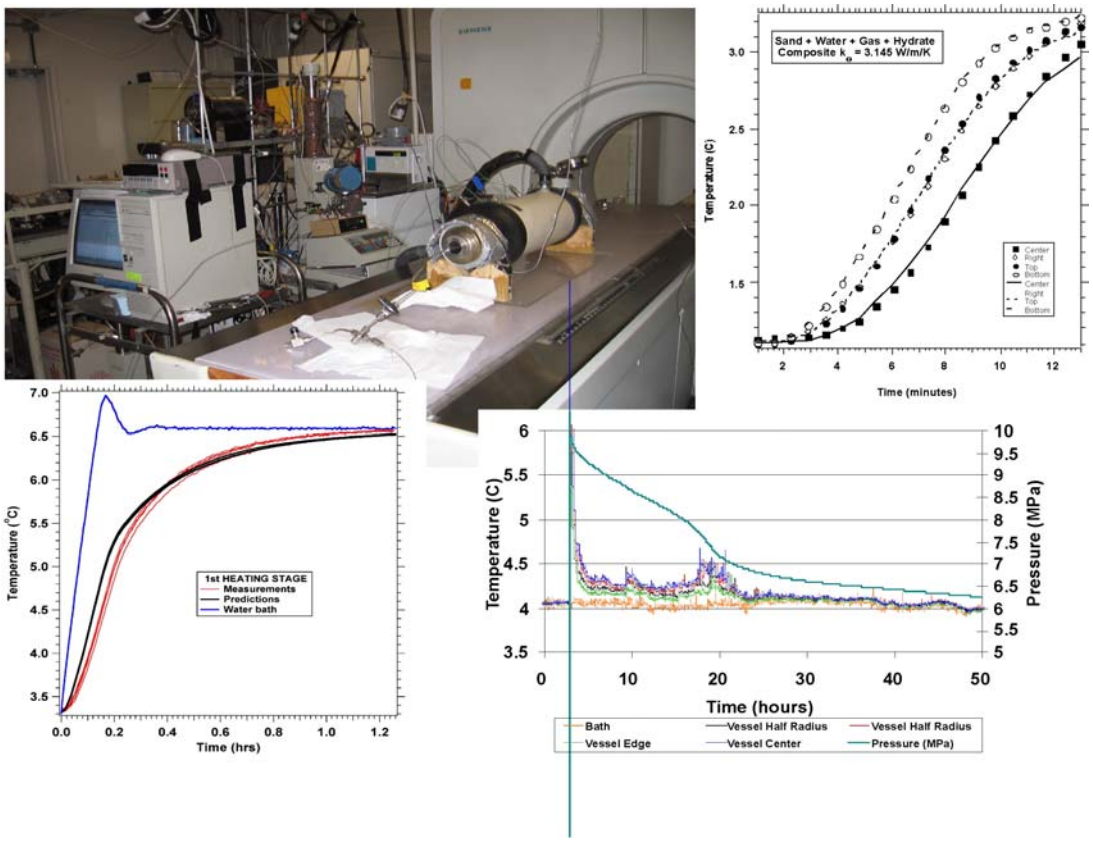

Fig. 7. Apparatus for concurrent hydrate thermal, kinetic and x-ray CT scanning studies; measurements and parameters obtained by history matching of the lab data.

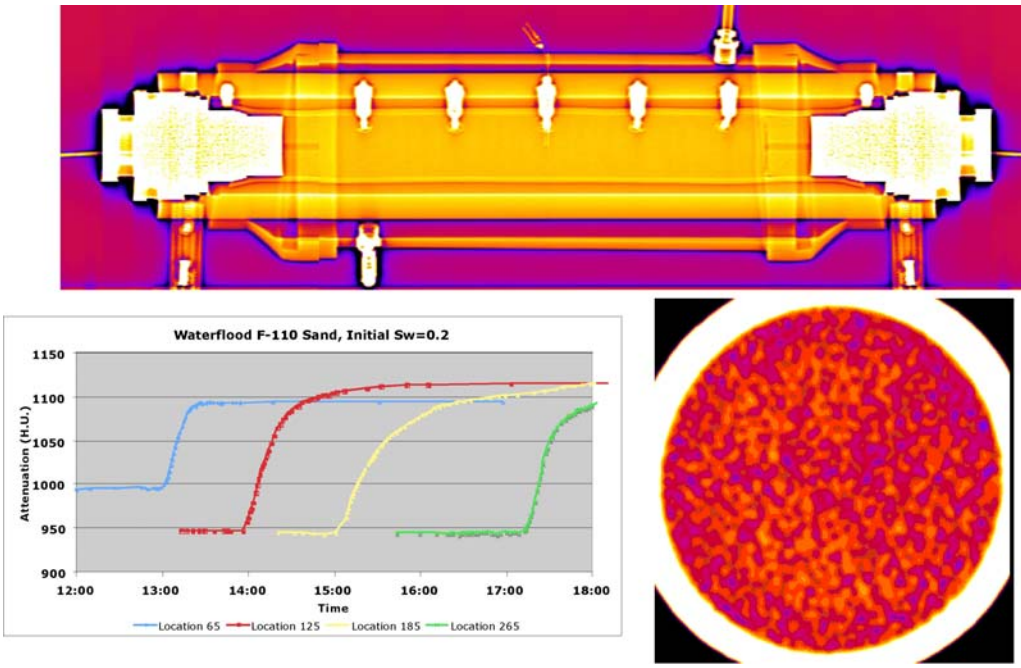

Fig. 8. Apparatus for concurrent relative permeability and x-ray CT scanning studies; attenuation curves (related to density), and cross-sectional scan of the evolving sample density during waterflooding (data used to extract the relative permeability curves).

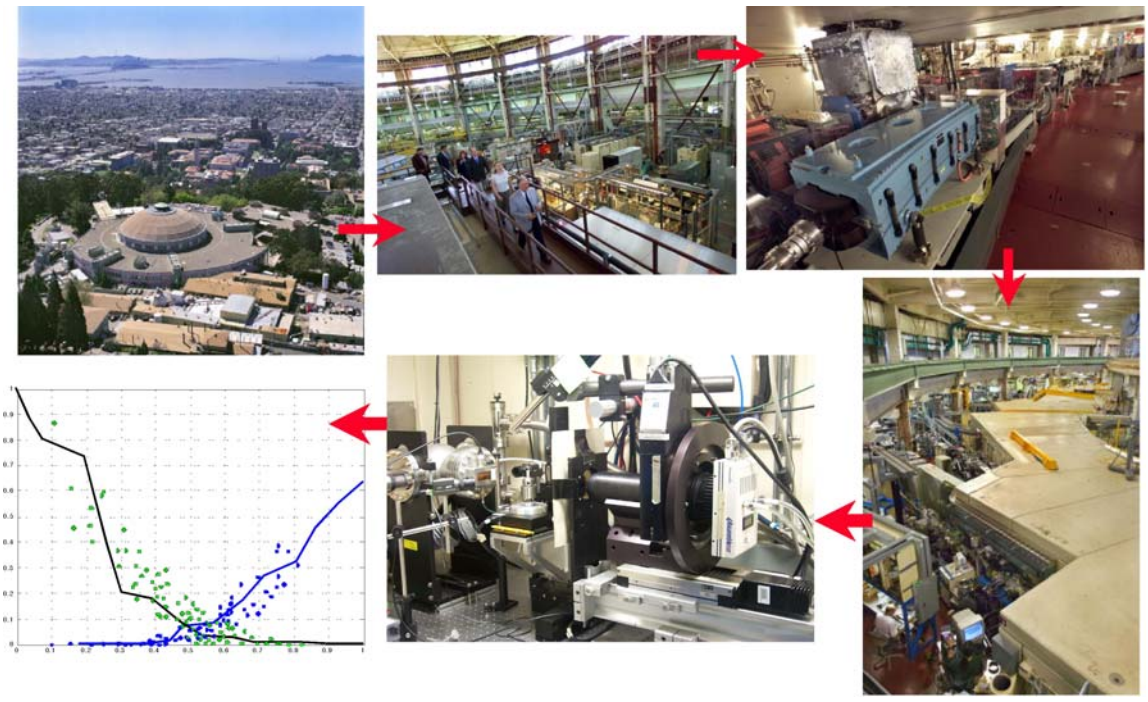

Fig. 9. The Advanced Light Source at LBNL, and use of the Beamline 8.3.2 to derive by means of x-ray microtomography relative permeability and capillary pressure relationships of hydrate-bearing media based on pore structure data.

5. SUMMARY

We discuss the range of activities at Lawrence Berkeley National Laboratory in support of gas production from natural hydrates. Numerical simulation of depressurization-induced gas production indicates that Class 1 and 2 hydrate deposits hold significant promise as potential energy sources because they can yield large gas volumes at high rates using conventional production technology. In Class 3 deposits, neither pure depressurization (when S_H is sufficiently low to permit significant flow) nor thermal stimulation (when S_H >70%, thus severely reducing permeability) results in commercially viable gas production. Class 4 deposits are not promising production targets. We developed a laboratory program (closely coordinated with the simulation studies) to obtain parameters and relationships describing the thermal, thermodynamic, hydraulic and kinetic properties of hydrate-bearing media that are important in predicting gas production. An important feature of the laboratory studies is the use of x-ray CT scanning and microtomography to describe the strong spatial and temporal heterogeneity of hydrates in porous media. Finally, we discuss briefly the LBNL studies in support of field tests of gas production from hydrates.

ACKNOWLEDGMENTS

This work was supported by the Assistant Secretary for Fossil Energy, Office of Natural Gas and Petroleum Technology, through the National Energy Technology Laboratory, under the U.S. Department of Energy, Contract No. DE-AC03-76SF00098. The authors are indebted to John Apps and Dan Hawkes for their thorough review and their insightful comments.

REFERENCES

Sloan, E.D., 1998, *Clathrate Hydrates of Natural Gases*, Marcel Dekker, Inc., New York, NY.

Gupta, A., T. Kneafsey, G.J. Moridis, Y. Seol, M.B. Kowalsky, and E.D. Jr. Sloan, 2006 *Methane hydrate thermal conductivity in a large heterogeneous porous sample, J. Phys. Chem. B,*10.1021/jp0619639 (LBNL-59088).

Kneafsey, T., L. Tomutsa, G.J. Moridis, Y. Seol, B. Freifeld, C.E. Taylor and A. Gupta, *Methane hydrate formation and dissociation in a core-scale partially saturated sand sample*, In Press, *J. Petr. Sci. Eng.*, (LBNL-59087, 2005).

Moridis, G.J. and T.S. Collett, 2003, *Strategies for gas production from hydrate accumulations under various geologic conditions*, LBNL-52568, Lawrence Berkeley National Laboratory, Berkeley, CA.

Moridis, G.J., T.S. Collett, S.R. Dallimore, T. Satoh, S. Hancock and B. Weatherhill, 2004, Numerical studies of gas production scenarios from several CH_4-hydrate accumulations at the Mallik site, Mackenzie Delta, Canada", *J. Petr. Sci. Eng.*, Vol. 43, 219-238.

Moridis, G.J., M.B. Kowalsky and K. Pruess, 2005a, *TOUGH-Fx/HYDRATE v1.0 User's Manual: A code for the simulation of system behavior in hydrate-bearing geologic media*, LBNL-58950, Lawrence Berkeley National Laboratory, Berkeley, CA (2005).

Moridis, G.J., M.B. Kowalsky and K. Pruess, 2005b, *Depressurization-induced gas production from Class 1 hydrate deposits*, SPE 97266, 2005 SPE Annual Technical Conference and Exhibition, Dallas, Texas, U.S.A., 9 – 12 October 2005.

Moridis, G.J., Y. Seol and T. Kneafsey, 2005c, *Studies of reaction kinetics of methane hydrate dissociation in porous media*, Paper 1004, Proc. 5th International Conf. on Gas Hydr., 21-30 (LBNL-57298).

Moridis, G.J., T.S. Collett, S.R. Dallimore, T. Inoue and T. Mroz, 2005d, *Analysis and interpretation of the thermal test of gas hydrate dissociation in the JAPEX/JNOC/GSC Mallik 5L-38 gas hydrate production research well*, Geological Survey of Canada, Bulletin 585, S.R. Dallimore and T. Collett, Eds., (LBNL-57296).

Moridis, G.J. and M. Kowalsky, 2006, *Gas production from unconfined Class 2 hydrate accumulations in the oceanic subsurface*, Chapter 7, in Economic Geology of Natural Gas Hydrates, M. Max, A.H. Johnson, W.P. Dillon and T. Collett, Eds., Kluwer Academic/Plenum Publishers, 249-266 (LBNL-57299).

Moridis, G.J. and E.D. Sloan, 2006, *Gas production potential of disperse low-saturation hydrate accumulations in oceanic sediments*, LBNL-52568, Lawrence Berkeley National Laboratory, Berkeley, CA.